

Molecular Cloning and Partial Characterization of a Plant VAP33 Homologue with a Major Sperm Protein Domain

Franck Laurent,¹ Gilles Labesse,² and Pierre de Wit³

Laboratory of Phytopathology, Wageningen University, Binnenhaven 9, 6709 PD Wageningen, The Netherlands

Received February 16, 2000

In a search for proteins interacting with the resistance protein Cf9 from tomato, a new cDNA was cloned and characterized. Protein sequence database searches suggested that the 120 residue-N terminal domain of the encoded protein (named VAP27) is highly similar to the VAP33 protein family from animals, to uncharacterized plant proteins, and to a lower extent, to the major sperm protein (MSP) from nematodes. The second half of the protein is similar to VAMP and to the VAP33 N-terminus comprising a predicted coiled-coil region followed by a transmembrane segment. The sequence/structure comparison of VAP27 with the crystal structure of AsMSP1 from *Ascaris suum*, using molecular modeling with the threading method, suggested that the N-terminus of VAP27 does possess a MSP-like domain that might participate in the formation of a protein-protein network. The coiled-coil region of VAP27 was modeled based on the structure of the VAP- and VAMP-containing SNARE complex. The coiled-coil region might also be involved in protein-protein interactions similar to VAP-VAMP interactions. © 2000 Academic Press

Key Words: homology modeling; structure/function analysis; membrane trafficking; membrane protein; transport protein; Cf-9; MSP.

The interaction between the fungal pathogen *Cladosporium fulvum* and its only host tomato complies with the gene-for-gene model. Many avirulence genes

in the pathogen and many matching resistance genes in the host have been identified (reviewed in 1). The matching gene pair *Avr9/Cf-9* has been studied in much detail (1). Thus, the *Avr9* gene from the fungus is the only genetic component necessary for the elicitation of active defense responses (including the hypersensitive response) in tomato plants carrying the corresponding *Cf-9* gene. These responses eventually result in resistance. The *Cf-9* encoded protein belongs to the class 4-resistance protein family, which contains membrane proteins with extracellular LRRs and a short cytoplasmic tail (2). Although for the activation of defense responses both *Avr9* and *Cf-9* are required, so far we have failed to prove that their encoded proteins directly interact by using the yeast two-hybrid assays and *in vitro* biochemical analysis. In addition to our attempts to prove direct interaction between *Avr9* and *Cf9* by using the yeast two-hybrid system, we have been searching for plant proteins interacting with the *Cf9* protein which could be involved in the signal transduction cascade leading to the induction of plant defense responses. In addition to activation of proteins, various mechanisms of protein secretion and protein transport might be involved in the expression or activation of plant defense responses.

An interesting example of such a mechanism is the VAP33 protein family, first described in *Aplysia californica* (3) as a member of the SNARE complex involved in vesicular docking and neurotransmitter exocytosis in nervous cells. VAP33 is a presynaptic plasma membrane protein that interacts specifically with VAMP, a vesicle membrane protein (3). This specific interaction would be responsible for anchorage and fusion of the synaptic vesicle to the plasma membrane. VAP33 homologues have also been isolated from yeast and mammals (4, 5). Expression studies in mammals show that their presence is not restricted to nervous cells suggesting that this complex may participate in more general aspects of membrane trafficking (4, 34, 35). It is anticipated that similar mechanisms also occur in plants. Homologues of several SNARE proteins (not VAP33 so far) have been identified in plants

Abbreviations used: aa, amino acid; HCA, hydrophobic cluster analysis; MSP, major sperm protein; VAMP, vesicle-associated membrane protein; VAP33, VAMP-associated protein of 33 kDa; His, histidine; Ade, adenine; Leu, leucine; Trp, tryptophan; LacZ, β -galactosidase encoding gene.

¹ Present address: Laboratoire de Biologie du Développement des Plantes, Institut de Biotechnologie des Plantes, Université Paris-Sud, Bat. 630, 91405 Orsay Cedex, France.

² Centre de Biochimie Structurale, CNRS UMR C9955, INSERM U414, Université Montpellier I, 15 avenue Charles Flahault, F-34060 Montpellier Cedex 2, France.

³ To whom correspondence should be addressed. Fax: 31-317-483412. E-mail: Pierre.deWit@medew.fyto.wau.nl.

through sequence identity, immunological relatedness or by complementation of yeast transport protein mutants (reviewed in 6 and 7). Moreover, it has been shown that specific SNAREs are involved in all steps of secretion, from the endoplasmic reticulum to the plasma membrane or the vacuole (7). These findings support the hypothesis of a system universally used in eucaryotic cells for intracellular transport, secretion and endocytosis (6, 8, 9).

Another example of cellular movement mechanism implies the Major Sperm Protein (MSP) from nematodes. Unlike most animal sperm, which is flagellated, nematode sperm cells are amoeboid and crawl in a solid substrate via an extended pseudopod (10, 11). This unique motility system resembles that of all crawling cell types except that they contain no actin but MSP, a small protein (14 kDa) that polymerizes into filamentous network. No homologues of MSP have yet been found in other cell types of nematodes or other animals (10). Nevertheless, *in vitro* studies have shown that MSP can trigger the movement of membrane vesicles (10).

Usually straightforward in cases of high sequence identity (over 35%), the alignment of all the sequences belonging to the same structural family with conventional homology search programs (12) becomes more hazardous and tedious at low sequence identity level (below 25%) (13). Additional methods for correct gathering and alignment of sequences are available for the analysis of a new protein sequence belonging to a given structural family (14, 15). Furthermore, the correct conservation of the three-dimensional structures may lead to the identification of a distantly related homologue from an already determined three-dimensional structure (16). Such an approach, with a careful analysis of the deduced structural model has shown to be helpful for the determination of specific functional features in spite of the low sequence identity (16, 17). Thus, by combining both a refined alignment and a three-dimensional structure analysis, comparative molecular modeling may facilitate the experimental characterization of new homologues.

In this work, we have used the yeast two-hybrid system to identify proteins interacting with the Cf9 protein encoded by the resistance gene *Cf-9*. We report in this paper the structure/function analysis of a new VAP protein (VAP27) at the molecular level. The corresponding cDNA was cloned and sequenced from a cDNA library from *Nicotiana plumbaginifolia*. Protein sequence database searches (12) reveal that VAP27 is the first member of the VAP33 family identified in plants. We also show that VAPs do contain a MSP-like domain (N-terminal half) associated to a VAMP domain (C-terminal half). However, we could not deduce directly its precise function due to the low sequence identity level. The putative function of this new protein was investigated using both a comparative molecular

modeling with the crystal structure of AsMSP1 (18, 19) and that of a SNARE complex comprising the soluble part of a VAMP (20). A putative function of VAP27 in membrane trafficking and Cf9-dependent resistance is discussed.

MATERIALS AND METHODS

Yeast and bacterial strains. The library screening was performed in yeast strain PJ69-4A (*MATa trp1-901 leu2-3,112 ura3-52 his3-200 gal4Δ gal80Δ LYS2::GAL1-HIS3 GAL2-ADE2 met2::GAL7-LacZ*) constructed by James *et al.* (21). Reporter genes carried by this strain are HIS, ADE and LacZ. Yeast double transformants were grown on SD medium (yeast nitrogen base without amino acids 6.7 g/l) supplemented with the appropriate dropout solution lacking Leu and Trp.

Positive vectors were electroporated and produced in KC8 (*hsdR, leuB600, trpC9830, pyrF::Tn5, hisB463, lacΔX74, strA, galU, K*).

Construction of fusion vectors and DNA manipulation. Vectors used in this study are yeast two-hybrid system vectors pGBT9 and pGAD10 carrying LEU and TRP as marker genes, respectively (CLONTECH Laboratories, Inc.). The cDNA library was fused to the activation domain (AD) of GAL4 in vector pGAD10 and was kindly provided by Thomas Heizel (Basel). The bait plasmid was constructed as follows: the C-terminus of *Cf-9* (EFG domain) (2) was PCR amplified using *Pfu* polymerase according to the manufacturer's instructions (Stratagene) and primers FLC3 (AAATGAATTCGAA-GATCAAGTGACAAC) and FLC2 (TTATAGTCGACCTAATATCTT-TTCTTGTCG) carrying an *EcoRI* and *SalI* restriction site, respectively. The amplified band was digested with the appropriate restriction enzymes and fused to the binding domain of GAL4 (BD) in the *EcoRI* and *SalI* sites of pGBT9, giving vector pBD-EFG. Restriction enzymes and T4 ligase were from GibcoBRL. Primers were synthesized by Amersham-Pharmacia.

Library screening. Bait vector and prey cDNA library vectors were sequentially transformed in PJ69-4A according to Ausubel *et al.* (22). Positive transformants were selected on SD-Trp-Leu-Ade medium. Positive colonies were screened for His and LacZ reporter genes expression. X-Gal assay was performed as previously described (23). The size of the cDNA insert was determined by direct colony PCR on yeast clones.

Isolation and sequencing of plasmid DNA. Plasmid DNA was isolated from yeast strains as described by CLONTECH. Positive pGAD10-X vectors were transferred to and produced in strain KC8. Transformant strains were selected on M9 minimum medium (24) lacking Trp.

Plasmid vectors were isolated from these clones using the Qiagen miniprep kit. Positive cDNAs were sequenced using primers G4ADF (TATTCGATGATGAAGATACCCACCAACC) and G4ADR (AAG-TGAAGTTGCGGGGTTTTTCAGTATCTACG) located on both sides of the cloning sites in opposite orientation.

Protein sequence comparison and molecular modeling. Protein sequence database searches were performed with the programs BLAST 2.0.9 and PSI-BLAST 2.0.5 (12) with default parameters. Sequence alignments and secondary structure predictions were performed by Hydrophobic Cluster Analysis (HCA) as previously described (14, 17). MultiCoil (25) and PAIRCOIL (26) were used to confirm the putative coiled-coil region. Alignment refinement was subsequently performed using the program TITO (16) where the AsMSP1 (18; PDB1MSP) and the SNARE complex (20; PDB1SFC) were used as a template for the N-terminus and the C-terminus, respectively. Three-dimensional models were built using MODELLER 4.0 (27) and assessed with Verify3D (28). These three-dimensional structures were visualized on a UNIX workstation using Xmol (29).

AAT	CGC	TTC	TCC	GGC	CGA	TTA	GCA	AAT	CGG	GTC	GGA	ATG	AGT	AAC	GGC	GGT	GGA	54
N	R	F	S	G	R	L	A	N	R	V	G	M	S	N	G	G	G	6
GAG	CTA	CTT	CAA	ATC	GAG	CCT	CTT	GAG	CTT	CAG	TTT	CCC	TTT	GAA	TTG	AAG	AAG	108
E	L	L	Q	I	E	P	L	E	L	Q	F	P	F	E	L	K	K	24
CAG	ATC	TCA	TGC	TCC	ATA	CAG	TTG	ACA	AAC	AAG	TCC	GAT	AAC	TAT	GTC	GCT	TTC	162
Q	I	S	C	S	I	Q	L	T	N	K	S	D	N	Y	V	A	F	42
AAG	GTG	AAG	ACG	ACG	AAT	CCA	AAG	AAA	TAT	TGT	GTA	AGG	CCC	AAC	ACT	GGA	GTT	216
K	V	K	T	T	N	P	K	K	Y	C	V	R	P	N	T	G	V	60
GTC	ATG	CCT	CAC	TCT	GCC	AGC	GAT	GTC	ATA	GTT	ACA	ATG	CAA	GCA	CAG	AAG	GAG	270
V	M	P	H	S	A	S	D	V	I	V	T	M	Q	A	Q	K	E	78
GCT	CCA	GCA	GAC	ATG	CAA	TGC	AAG	GAT	AAG	TTC	CTG	CTT	CAA	AGT	GTT	GTT	GCA	324
A	P	A	D	M	Q	C	K	D	K	F	L	L	Q	S	V	V	A	96
AGC	CCT	GGC	GCT	ACT	GCA	AAG	GAC	ATT	ACT	CCT	GAG	ATG	TTC	AAT	AAG	GAG	GAG	378
S	P	G	A	T	A	K	D	I	T	P	E	M	F	N	K	E	E	114
GGG	AAT	CAT	GTG	GAG	GAT	TGT	AAG	TTG	AGA	GTC	ATT	TAC	GTT	CCA	CCT	CAA	CAA	432
G	N	H	V	E	D	C	K	L	R	V	I	Y	V	P	P	Q	Q	132
CCA	CCA	TCG	CCG	GTG	CAG	GAG	GGT	TCC	GAG	GAA	GGT	TCC	TCT	CCT	AGG	GCC	TCA	486
P	P	S	P	V	Q	E	G	S	E	E	G	S	S	P	R	A	S	150
GTG	TCT	GAA	AAT	GGA	GCT	GTA	AAT	ACA	TCC	GAG	TTT	AAT	AAT	ATT	TCA	AGG	GCA	540
V	S	E	N	G	A	V	N	T	S	E	F	N	N	I	S	R	A	168
TAT	AAT	GAG	CAG	CAA	GAC	AGC	TCG	TCG	GAG	ACA	AAG	GCA	CTA	ATT	TCA	AAG	CTG	594
Y	N	E	Q	Q	D	S	S	S	E	T	K	A	L	I	S	K	L	186
ACA	GAG	GAG	AAA	ATT	TCT	GTT	ATA	CAG	CAA	AAT	AAC	AAG	CTT	CAG	CAA	GAA	TTG	648
T	E	E	K	I	S	V	I	Q	Q	N	N	K	L	Q	Q	E	L	204
GCG	CTC	TTG	AGA	CGT	GAA	CGT	AAC	AGT	AGT	CGT	GGT	GGG	ATC	CCA	ACT	ATA	TAT	702
A	L	L	R	R	E	R	N	S	S	R	G	G	I	P	T	I	Y	222
GTT	CTC	ATT	ATT	GGA	TTG	CTG	GGC	ATC	ATT	CTG	GGC	TAT	CTT	CTA	AAA	AAG	ACA	756
V	L	L	L	G	L	L	G	L	L	G	Y	L	L	L	K	K	T	240
TAA	TCA	TTT	AGA	CAA	CCT	TGA	TAT	ATT	CTC	AAT	GCT	CCA	ACT	GTT	TGA	AAA	ACT	810
*																		
TCA	GAA	TCT	AAA	GTC	AAT	TAG	TTG	TCT	GGT	TGA	CTT	GAC	TTT	TCT	ACA	AGT	CAC	864
TTT	CAT	TGG	CTT	TGT	AAT	GTG	GCC	TAG	AGC	TTC	AAG	AGC	TAT	CAT	CAT	CTG	GCC	918
TAC	TAT	ATC	GAC	ATC	CTC	CTT	TTG	GCA	ATT	TGA	GAA	GAC	AAC	ATT	AGT	TTA	TTG	972
ATC	AAA	GTG	TAC	TTC	CTA	AGT	TAT	GGC	TGC	GAC	AAA	GTG	TTG	GAA	ATA	CTG	ATA	1026
AGT	GAT	TGT	AGT	TGA	GTG	ATC	CTA	ATG	GCA	TGG	GGG	ATT	TAC	CTG	GAG	TAC	TTC	1080
AAC	TGT	TTT	CCT	TGG	TTA	CCC	TTG	GAG	ACC	TTA	TTT	TCG	TTT	TTA	GAT	TTT	ATC	1134
TTG	TTT	GCG	CCT	TTT	TCT	GTA	TTT	TTT	GGG	GTT	GTT	TGA	TTG	ACC	ATA	TTA	CAT	1188
ATA	ATC	TCA	GTA	CTA	AAG	TTC	GTG	CTA	AAA	AAA	GTC	GAC	GCG	GCC	GCG	AAT	TC	1241

FIG. 1. Nucleotide sequence of clone 27-6 (EMBL AJ251365) and deduced amino acid sequence of VAP27. Numbering of the bases and amino acids are shown on the right. The putative starting codon is in bold. Amino acids in italic are not considered in the peptidic sequence. The coiled-coil region is boxed and the transmembrane domain is dash-boxed.

RESULTS

Isolation and Characterization of the 27-6 cDNA

The cDNA clone 27-6 was isolated twice by a yeast two-hybrid screen using the C-terminal EFG domain (2) of the tomato resistance gene *Cf-9*. The E-domain is supposed to be extracellular, the F-domain represents the transmembrane segment, while the G-domain is cytoplasmic. This interaction was confirmed for the three reporter genes present in the yeast strain. Moreover, both fusion vectors failed to induce the expression of the reporter genes when transformed alone or together with the empty other vector. However, the cDNA 27-6 and the EFG domain of *Cf-9* failed to interact when swapped in both two-hybrid vectors (i.e. 27-6

cDNA fused to the binding domain and EFG fused to the activation domain). This step is often performed to eliminate false-positive interactions where the interaction is due to a nonspecific structure of the fusion proteins. However, swapping can also give rise to fusion proteins presenting particular characteristics (instability, aggregation) preventing specific interaction. The specific interaction of EFG or the complete *Cf-9* protein with the 27-6 encoded protein will thus have to be confirmed biochemically. Furthermore, Northern analysis using cDNA 27-6 as a probe showed that the expression of the corresponding gene is constitutive after challenge of *Cf-9* plants with Avr9 (data not shown).

Clone 27-6 is 1241 base pairs long (Fig. 1) and does

UPROT	***-----**T*D*VD*****LY*G**T*****	55
VAP27	MSNGG--GELLQIEPLELQFPFELKKQISCSITQLTNKSDNYVAFVKVTNPKKYCVRPNT	58
VAP33	*AKHE--QI*VLDP*TD*K*KGPF*TDVV*TNLK*R*P*RK*C*****A*RR*****S	58
MSP1	*AQSVPP*DINTQPSQKIV*NAPYDDKHTYH*KI**AGRRIGWAI****MRRLS*D*PC	60
UPROT	***H*R*S*E*L*****L*****C*****P**V*H**S**A*HR*	115
VAP27	GVMFPHSASDVIITMQAQKEAPADMCKDKFLLQSVVASPGATAKDITPEMFNKEEGNHV	118
VAP33	**IID*G*TVT*S*ML*PFDYD*NE-KS*H**MV*TF*P*NTSDMEAVWKEAKPD*---L	114
MSP1	**LD*KEKVLMA*SCDTFNA*TE*LN--NDRITIEWTNT*DGA**QFRR*W*QGDG--M*	116
UPROT	*ET***V**A*PR*****R*****D*--*A*D*TAAP*FSADRVDA**N	173
VAP27	EDCKLRVIYVPPQPPSPVQEGSEEGSSPRASVSENGAVNTSEFNISRAYNEQ---QDS	175
VAP33	M*S***CVFEM*NENDKLNDEPSKAVPLN**KQDGPMPKPHSVSLNDTETRKLMEECKR	174
MSP1	RRKN*PIE*NL 127	
UPROT	*AR**VT*****N*AV*L**R*****DO****SKR*KS***FM***LV**I*L***	233
VAP27	SSETKALISKLTTEEKISVIOQNNKLOQLALLRRERNSSRGGIPTIYVLIIGLLGIILG	234
VAP33	LOGEMMKL*EENRHLRDEGLRLR*VAHSDKPGSTSTA*FRDNVTSPLPSLLVVIAAIFIG	236
UPROT	*IM*R* 239	
VAP27	YLLKKT 240	
VAP33	FFLKFFIL 242	

FIG. 2. Multiple sequence alignment of VAP27 with highly homologous sequences: UPROT, unknown protein from *A. thaliana* (AC007659_5); VAP33, human homologue (AF044670); MSP1, AsMSP1 from *A. suum* (P27439). The multiple sequence alignment was performed using CLUSTALX and was improved using the structure/sequence comparison performed using the program TITO. Identities with VAP27 residues are shown with dashes and similarities are bold. Conserved positions in all four sequences are boxed in grey. The numbering of each sequence is shown on the right. The MSP domain detected by SMART is upperlined, coiled-coil regions are boxed and transmembrane domains are dash-boxed.

not present the features of a complete cDNA. Moreover, the cDNA band detected during a Northern analysis is 1380 bp long. However, the sequence of clone 27-6 presents an ATG in position 37–39. Additional informations obtained from sequence comparisons (see below) led us to conclude that despite the fact that the cDNA is incomplete, the coding region is most probably complete. In the following, the ATG at positions 37 to 39 will thus be considered as the start codon (Fig. 1).

The putative encoded protein containing 240 residues was named VAP27 and presents an expected molecular mass of 26.5 kDa. A specific feature of VAP27 is the presence, at its C-terminus, of a strongly hydrophobic stretch of 22 residues, which could represent a transmembrane segment, suggesting that VAP27 is a membrane protein. A coiled-coil region was also predicted upstream the transmembrane domain (Fig. 1). No typical signal or targeting sequence was observed in this sequence. According to the P-sort program, VAP27 is likely to be a reticulum or plasma membrane protein with its N-terminal domain being cytoplasmic.

Sequence Comparison

Sequence database screening using the VAP27 peptidic sequence as a query was first performed on both *A. thaliana* protein sequences (BLASTP on Atdb) and higher plants translated DNA sequences (TBLASTN). More than 30 plant sequences showed a high homology with VAP27, the best score being against an unknown protein from *A. thaliana* (AC007659, Fig. 2) with a

probability of 6.0×10^{-86} and an homology of 204 over 240 residues. Most of these sequences have been determined from cDNAs or BACs and are not annotated or encode putative or unknown proteins. All these proteins are yet uncharacterized except for MAMI-30 from *A. thaliana* (U83655; 30) which is induced by osmotic stress and is membrane-associated.

When VAP27 was compared to a nonredundant sequence database, best scores were obtained with the same *A. thaliana* unknown protein sequences. Additional high scores were obtained with the vesicle-associated membrane protein (VAMP)-associated protein family VAP33 from mammals and *A. californica* (Fig. 2). The yeast inositol regulator SCS2 (31) is also highly homologous to VAP27. All plant homologues, VAPs and SCS2 sequences share in their N-terminus a common highly conserved domain (120 residues, Fig. 2). This supported the choice of the starting codon in VAP27. More distantly related to VAP27 are the major sperm proteins (MSP) from nematodes. The homology spans the N-terminus of VAP27 and about the complete sequence of MSP (127 residues). The first hit was with a MSP from *Caenorhabditis elegans* (U23519) with an E value of 7×10^{-25} and 22% identity and 41% homology over 94 residues.

Similar similarity values have already been observed when comparing SCS2 or VAP33 homologues with MSPs (3, 4, 31). However, these were seen as inconclusive due to their low sequence identity. Furthermore, known MSP are soluble proteins while

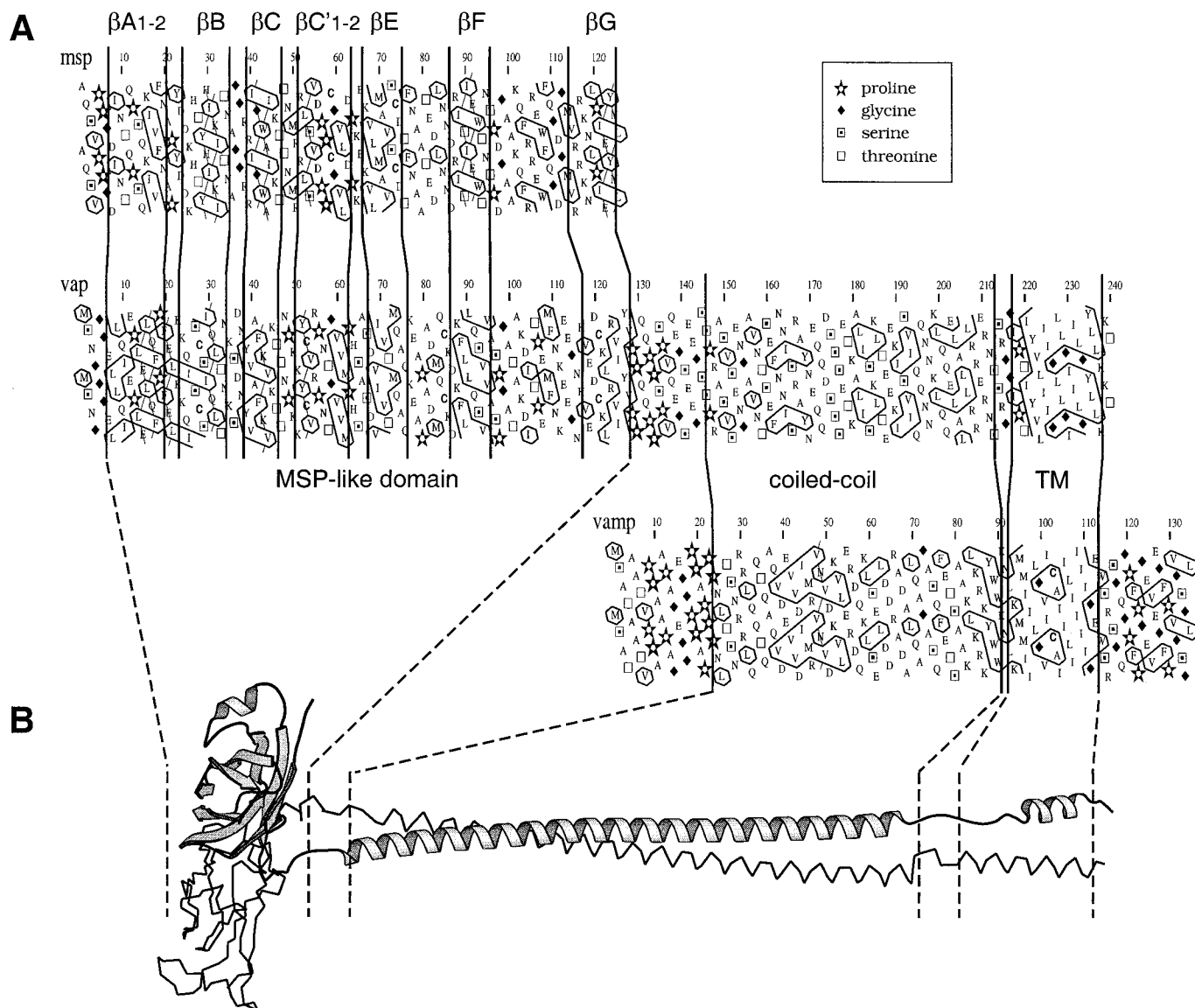


FIG. 3. (A) Alignment of the HCA plot of the sequences of AsMSP1 (msp), VAP27 (vap) and VAMP (vamp). Predicted secondary structure conservation is highlighted with plain bars. (B) Modeled structure of VAP27. The molecular model was deduced from the structure/sequence comparison performed using the program TITO and analyzed using the visualization program XmMol. It shows the conserved tertiary structures in the Ig-like core, coiled-coil region and transmembrane domain delineated with dashed bars. Thick arrows on (B) represent the β -strands.

VAP27 and its homologues are predicted or demonstrated (3, 30, 31) membrane or membrane-associated proteins.

In order to confirm this primary sequence comparison, we performed multiple sequence alignment and secondary structure predictions using Hydrophobic Cluster Analysis (HCA) (14). This analysis suggested the conservation of the same fold for both the VAP27 and the AsMSP1 molecules (Fig. 3), derived from the so-called Ig-fold (32). Despite small insertions or deletions of a few amino acid residues in length, the secondary structure elements of AsMSP1 appeared conserved through HCA in VAP27 (Fig. 3A). Similarly, the

coiled-coil region and the transmembrane segment were assigned by prediction using PAIR-Coil, Multi-Coil and HCA as well as by sequence comparison for example with VAMP despite the very low sequence identity. We further investigated these sequence comparisons to check for the existence of a stable MSP domain in VAP.

Structure/Function Relationship

To ensure the proper alignment of the VAP27 sequence with the MSPs, a previously described strategy using the software TITO was applied (16). This allows

a rapid and simultaneous analysis of a multiple sequence alignment, and it measures the compatibility of the aligned sequences with a known three-dimensional structure. The recently solved crystal structure of AsMSP1 (18, 19) was used as a template despite the low sequence identity (20% over 125 aa). TITO pseudo-energy (16) validated the proposed alignment (Fig. 2) of the VAP27 sequence and the AsMSP structure (E_{total}: -26.6 per aligned residues in the monomer). Based on the refined alignment, a three-dimensional model was built using MODELLER 4.0 (27) and checked using the program Verify3D (28). The global score (residues 1–120) in Verify3D reaches ~0.3 (versus ~0.5 for the crystal AsMSP structure). These values suggest, in spite of the low sequence identity level, that the proposed fold is correct. AsMSP1 is composed of one Ig-like domain comprising oligomerization interfaces as observed in the crystal structures (18). In the VAP27 model, the structure core is mainly composed of hydrophobic residues. Four cysteines occupied distant positions either on the surface (C53 and C85) or in the interior of the structure (C28 and C121). No disulfide bridge is predicted to stabilize the fold. In MSP, the very C-terminus and the first strand are involved in a side-by-side dimerisation as deduced from the PDB1MSP crystal packing. Based on the sequence comparison this dimerisation interface is proposed to be conserved. In VAP27, it would comprises the residues 11 to 21, 128 to 129 and the glutamine Q31. The buried amino acids observed at the interface in the deduced dimeric model are mainly hydrophobic except for glutamine Q17. In the monomer, these residues would be solvent exposed. The glutamine side-chain is buried in the center of the hydrophobic patch and is predicted to form stable hydrogen bonds with its counterpart (Q17') upon dimerisation. Surrounding this patch, salt bridge or hydrogen bonds (K23-K24-E21-Q31') are also predicted to further stabilize the dimer.

According to the second crystal form, MSP filaments form by successive multimerization of the previous dimer. The interface in MSP involves the very N-terminal end (aa 2 to 7) and a stretch of the last strand (aa 112–119). No major residue changes are observed according to our alignment. Little structural changes are predicted that would not alter the interface and prevent the oligomerization. Furthermore, the interaction of an MSP and VAP through this interface appeared feasible according to our model and the predicted sequence change.

Despite its strict conservation, the role of the motif KTTxN (aa 45–49 in VAP27) remains unclear. It is partially involved in the stabilization of the overall fold as the threonine side chains are hydrogen bonded to neighboring main chain atoms (residues N49, D87 and K88) while asparagine N49 side chain points toward the aspartate D87. A conserved tyrosine (Y127) also points toward this aspartate. A common MSP and VAP

partner might also recognize this conserved structural motif.

Similarly, the coiled-coil region was modeled onto the 3D structure of VAMP as observed in the SNARE complex PDB1SFC. However, the sequence identity is much lower (roughly 10%) and the particular helix-helix interaction in the coiled-coil render the comparative modeling more difficult. The helix fold was mainly deduced from the secondary structure prediction and the coiled-coil prediction. The predicted dimerisation of the MSP domain also supports a dimerisation of the coiled-coil region due to the very close spatial proximity of the C-terminus of the two associated globular domains. This makes that each helix forming the coiled-coil to start at close distance after the short proline-rich stretch.

However, our sequence and structure analysis cannot detect specific motifs leading to precise prediction of the quaternary structure of the coiled-coil region. Furthermore, the precise nature and number of the VAP27 partners are not known. The formation of homo- or heterodimers is necessary due to the presence of hydrophobic residues along the whole coiled-coil region. The SNARE complex structure indicates that further oligomerization also involves hydrophilic residues. Such interactions are likely to be conserved in VAP27 due to its sequence conservation with the other VAPs but cannot be shown without further experimental investigations.

The model suggests that VAP27 might form a dimer or a multimer in its N-terminus and a heterotetramer in its C-terminus (Fig. 3B).

DISCUSSION

The cloning and sequencing of a new cDNA from tobacco is presented here. VAP27 is the first VAP33-like protein identified in plants. We show here that the VAPs contain a MSP-like domain in their N-terminus. This is the first report on the occurrence of such a plant protein comprising both a MSP-like domain and a coiled-coil segment. VAPs are the only proteins reported so far that contain both a MSP-like domain and a VAMP-like domain (transmembrane domain and coiled-coil region). The refined structure/function analysis of VAP27 and *A. suum* MSP indicates that the residues involved in the fold core are conserved as well as the seven β -strands. MSP-dependent movement is unique for nematodes amoeboid sperm cells. It is structurally different from actin but mechanistically similar. MSP aggregation starts from the leading edge of the plasma membrane (10). The soluble MSP may thus interact with a plasma membrane protein such as VAPs through their MSP-like domain. This hypothesis is supported by our finding of uncharacterized peptidic sequences from *C. elegans* that contain an MSP domain but are much longer than the MSP domain itself

(U97007, 323 aa; U32305, 514 aa). Moreover two *C. elegans* peptidic sequences have been previously annotated as similar to VAP33 (AF024499, 374 aa) and SCS2 (Z70754.1, 304 aa). Alternatively, plants may produce soluble MSP-like proteins. Actually, we found in the Atdb database uncharacterized sequences that are homologous to MSPs with a similar length (gi|3738316, 149 aa; gi|3738318, 110 aa; gi|4982497, 120 aa). Our hypothesis is also supported by the recent discovery that a mouse VAP33 is associated with the endoplasmic reticulum and microtubules (36). Little is known about proteins interacting with the proteins encoded by resistance genes such as the Cf9 protein. VAP27 interacts with the EFG domain of Cf9, which codes for the C-terminal membrane localized domain of the protein. It is not known yet whether it interacts with the extracellular (E) or the intracellular domain (G). Immunoprecipitation using antibodies raised against Cf9 and VAP33-like proteins would be interesting to see whether both Cf9 and VAP27 will colocalize in membrane or microsomal fractions of Cf9 tomato plants. Induction of a plant VAP33 homologue under abiotic stress have been previously described (30). Moreover, other components of the vesicle trafficking machinery interact with the movement protein of the cauliflower mosaic virus (CaMV; 33). The role of the Cf9-VAP27 complex in defense responses or in signal transduction leading to plant defense after activation by the fungal peptide elicitor Avr9 is unknown yet. Nevertheless, our data confirm that this system, involved in protein trafficking and vesicle movement is widely occurring in eucaryotes and that MSP is not a unique system in nematode sperm. The VAPs might be a general link between vesicles and membrane component (VAMPs) to soluble components analogous to MSPs. According to this scheme, VAP27 will be an essential go-between vesicle motility and membrane fusion element.

ACKNOWLEDGMENTS

The authors thank Thomas Heizel for kindly providing the tobacco cDNA library, Tony van Kampen for sequencing, and Guy Honée for helpful discussion. This work was supported by ECC project No. CHRX-CT93-0168.

REFERENCES

- Joosten, M. H. A. J., and de Wit, P. J. G. M. (1999) *Annu. Rev. Phytopathol.* **37**, 335–367.
- Jones, D. A., Thomas, C. M., Hammond-Kosack, K. E., Balint-Kurti, P. J., and Jones, J. D. (1994) *Science* **266**, 789–793.
- Skehel, P. A., Martin, K. C., Kandel, E. R., and Bartsch, D. (1995) *Science* **269**, 1580–1583.
- Weir, M. L., Klip, A., and Trimble, W. S. (1998) *Biochem. J.* **333**, 247–251.
- Nishimura, Y., Hayashi, M., Inada, H., and Tanaka, T. (1999) *Biochem. Biophys. Res. Commun.* **254**, 21–26.
- Gal, S. (1998) in *Annu. Plant Rev "Arabidopsis"* (Anderson, M., and Roberts, J. A., Eds.), Vol. 1.
- Sanderfoot, A. A., and Raikhel, N. V. (1999) *Plant Cell* **11**, 629–641.
- Rothman, J. E. (1994) *Nature* **372**, 55–63.
- Bassham, D. C., and Raikhel, N. V. (1996) *Trends Plant Sci.* **1**, 15–20.
- Theriot, J. A. (1996) *Cell* **84**, 1–4.
- Smith, H. E., and Ward, S. (1998) *J. Mol. Biol.* **279**, 605–619.
- Altschul, S. F., Madden, T. L., Schaffer, A. A., Zhang, J., Zhang, Z., Miller, W., and Lipman, D. J. (1997) *Nucleic Acids Res.* **25**, 3389–3402.
- Sander, C., and Schneider, R. (1991) *Proteins* **9**, 56–68.
- Callebaut, I., Labesse, G., Durand, P., Poupon, A., Canard, L., Chomilier, J., Henrissat, B., and Mornon, J.-P. (1997) *Cell. Mol. Life Sci. (Experientia)* **53**, 621–645.
- Rost, B., and Sander, C. (1996) *Annu. Rev. Biophys. Biomol. Struct.* **25**, 113–136.
- Labesse, G., and Mornon, J.-P. (1998) *Bioinformatics* **14**, 206–211.
- Thoreau, V., Berges, T., Callebaut, I., Guillier-Gencik, Z., Greslin, L., Bernheim, A., Karst, F., Mornon, J.-P., Kitzis, A., and Chomel, J.-C. (1999) *Biochem. Biophys. Res. Commun.* **257**, 577–583.
- Bullock, T. L., Parthasarathy, G., King, K. L., Kent, H. M., Roberts, T. M., and Stewart, M. J. (1996) *Struct. Biol.* **116**, 432–437.
- Bullock, T. L., Roberts, T. M., and Stewart, M. (1996) *J. Mol. Biol.* **263**, 284–296.
- Sutton, R. B., Fasshauer, D., Jahn, R., and Brunger, A. T. (1998) *Nature* **395**, 347–353.
- James, P., Halladay, J., and Craig, E. A. (1996) *Genetics* **144**, 1425–1436.
- Ausubel, F. M., Brent, R. E., Kingston, R., Moore, D., Seidman, J. G., Smith, J., and Struhl, K. (Eds.) (1994) *Current Protocols in Molecular Biology*, pp. 13-7-1, J. Wiley and Sons, Inc., New York.
- Duttweiler, H. M. (1996) *TIG* **12**(9), 340–341.
- Sambrook, J., Fritsch, E. F., and Maniatis, T. (1989) *Molecular Cloning: A Laboratory Manual*, Cold Spring Harbor Laboratory, Cold Spring Harbor, NY.
- Wolf, E., Kim, P. S., and Berger, B. (1997) *Protein Sci.* **6**, 1179–1189.
- Berger, B., Wilson, D. B., Wolf, E., Tonchev, T., Milla, M., and Kim, P. S. (1995) *Proc. Natl. Acad. Sci. USA* **92**, 8259–8263.
- Sali, A., and Blundell, T. L. (1993) *J. Mol. Biol.* **234**, 779–815.
- Luthy, R., Bowie, J. U., and Eisenberg, D. (1992) *Nature* **356**, 83–85.
- Tuffery, P. (1995) *J. Mol. Graphics* **13**, 67–72.
- Galaud, J.-P., Laval, V., Carriere, M., Barre, A., Canut, H., Rouge, P., and Pont-Lezica, R. (1997) *Biochim. Biophys. Acta* **1341**, 79–86.
- Kagiwada, S., Hosaka, K., Murata, M., Nikawa, J.-I., and Takatsuki, A. (1998) *J. Bacteriol.* **180**, 1700–1708.
- Halaby, D. M., Poupon, A., and Mornon, J.-P. (1999) *Protein Eng.* **7**, 563–571.
- Huang, Z., Andrianov, V., and Howell, S. (1999) in 9th Int. MPMI Congress: Book of Abstracts, 138.
- Ding, B. (1998) *Plant Mol. Biol.* **38**, 279–310.
- Lapierre, L. A., Tuma, P. L., Navarre, J., Goldenring, J. R., and Anderson, J. M. (1999) *J. Cell Sci.* **112**, 3723–3732.
- Skehel, P. A., Fabian-Fine, R., and Kandel, E. R. (2000) *Proc. Natl. Acad. Sci. USA* **97**, 1101–1106.